

SECTORED TUBE-SHAPED IONIC POLYMER-METAL COMPOSITE ACTUATOR WITH INTEGRATED SENSOR

Marissa A. Tsugawa and Kam K. Leang*
Electroactive Systems and Controls Lab
Department of Mechanical Engineering
University of Nevada, Reno
Reno, Nevada 89557-0312, USA

Viljar Palmre and Kwang J. Kim
Active Materials and Processing Laboratory
Department of Mechanical Engineering
University of Nevada, Las Vegas
Las Vegas, Nevada 89154-4027, USA

ABSTRACT

This paper describes the development of a tube-shaped ionic polymer-metal composite (IPMC) actuator with sectored electrodes and an integrated resistive strain-based displacement sensor. Tube or cylindrical shaped IPMC actuators, with the ability to provide multiple degrees-of-freedom motion, can be used to create active catheter biomedical devices and novel bio-inspired propulsion mechanisms for underwater autonomous systems. An experimental tube-shaped IPMC actuator is manufactured from a 40-mm long Nafion polymer tube with inner diameter of 1.3 mm and outer diameter of 1.6 mm. The outer surface of the tube-shaped structure is plated with platinum metal via an electroless plating process. The platinum electrode on the tube's outer surface is sectored into four isolated electrodes using a simple surface milling technique. A custom-designed strain sensor comprised of 50 AWG ni-chrome wire is developed and attached to the tube's surface to sense the bending motion of the tube actuator. The integrated sensor is low cost and practical, and it avoids the need for bulky external sensors such as lasers for measuring deflection and feedback control. Preliminary experimental results are presented to demonstrate the performance of the IPMC tube actuator and integrated displacement sensor.

1 Introduction

Electroactive polymer materials, such as ionic polymer-metal composites (IPMCs), are active (smart) materials which

can be used to develop soft solid-state actuators and sensors [1]. IPMC-based actuators, for example, can produce large strain compared to other active materials such as piezoelectric ceramics. Additionally, they can be driven with low voltage (<5 V), are light weight, and can operate in an aqueous environment such as water, making them attractive for the development of novel biomedical devices and emerging bio-inspired underwater systems. For example, recent applications of IPMCs include biomedical tweezers [2], robotic snakes [3] or worms [4], micropump valves for microfluidic systems [5], and bio-inspired active fins for underwater robotics [6, 7].

Described herein is the fabrication of a tube-shaped IPMC actuator with sectored electrodes for realizing multiple degrees-of-freedom motion in a compact structure. The tube-shaped IPMC actuator is manufactured from a Nafion polymer tube with inner diameter of 1.3 mm and outer diameter of 1.6 mm, and the plated electrode on the outer surface of the tube is sectored into isolated electrodes using a simple surface machining process. In particular, the platinum electrode is sectored into four isolated electrodes, and electrical power is applied to each electrode for independent control of specific areas of the structure. By doing this, multiple degrees-of-freedom motion can be achieved, similar to sectored tube-shaped piezoelectric transducers [8].

To sense the deformation of the tube-shaped IPMC actuator, a custom-designed resistive strain sensor comprised of a 50 AWG ni-chrome (20% nickel and 80% chrome) wire is developed and strategically attached to the tube's outer surface to measure the tube's bending motion. It is pointed out that off-the-

*Corresponding author; Email: kam@unr.edu.

shelf strain sensors have recently been employed to measure the motion of IPMC strip actuators [9]. However, in this work the new strain sensor design is better suited for tube-shaped IPMC actuators and experimental results are presented to demonstrate proof-of-concept. The integrated sensor is low cost, compact, and practical. Such sensors also avoid the need for bulky external sensors such as lasers to measure displacement for monitoring and feedback control. For IPMC-based micro autonomous systems that require sensor feedback, compact integrated sensing schemes are highly desired. In the following, the fabrication of the tube-shaped actuator and integrated sensor is described in detail. Preliminary experimental results are presented to demonstrate the performance of the IPMC tube actuator and sensing scheme.

It is pointed out that compared to the proposed tube-shaped IPMC actuator, cantilever-shaped IPMC actuators (strip IPMC actuators) are the most commonly studied and used in applications. In this case, one end of a strip IPMC actuator is usually fixed and the actuator's bending motion is exploited, for example to create single-link [10] and multi-link [11] oscillatory propulsors. The fabrication of thick rectangular-shaped strip IPMC actuators using the simple hot-pressing method [12, 13] and casting process [14] to enhance actuation force have been developed. A combination of the hot-pressing and micromachining allowed the fabrication of IPMC tweezers with more complex shape [2].

Recently, there has been interest in IPMC actuators capable of multiple degrees-of-freedom motion for creating actuators and manipulators which can undergo complex motion and deformation. One way to achieve this is to pattern the electrodes on a strip IPMC actuator, and by applying voltages to each isolated electrode, multiple degrees-of-freedom motion such as twisting and bending motion can be achieved [15]. Multiple strip IPMC actuators were embedded into a soft boot structure to produce the similar bending and twisting behavior [7]. Disc-shaped IPMCs were created for sensing and energy harvesting applications [16]. Recently, cylindrical IPMC actuators were created for multiple degrees-of-freedom motion for applications such as active catheters [17]. By systematically creating electrodes on the surface of the polymer with proper electrical isolation between adjacent regions, a portion of the actuator can be independently controlled to achieve complex deformation while other regions can be used to *sense* the motion and deformation of the actuator [18]. The need to design IPMC actuators capable of multiple degrees-of-freedom motion motivated the work described herein.

2 IPMC Tube Actuator Fabrication Process

The basic IPMC actuator consists of an ion exchange polymer, such as perfluorinated alkenes or styrene/divinylbenzene-based polymers, sandwiched between two noble metallic electrodes as shown in Fig. 1. The electrode is typically platinum, but conducting media such as palladium, silver, gold, carbon, and graphite have been used. The metal electrodes are often

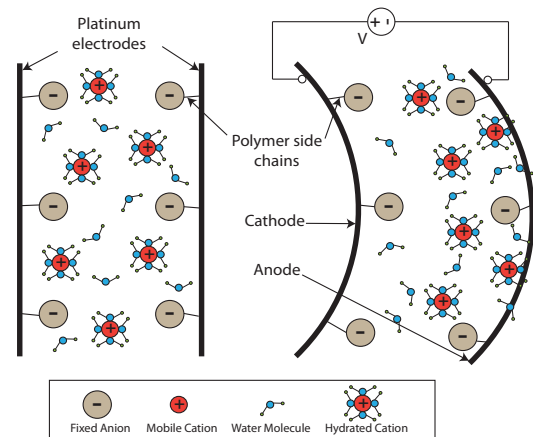


FIGURE 1. Illustrative movement of cations and water molecules inside of an IPMC material. When a voltage is applied, the mobile cations migrate to the anode which causes the membrane to swell leading to deformation of the IPMC [19].

chemically deposited on the polymer's surface through a reduction process [19]. When the composite material is saturated in a polar solvent (such as water) and then an electric field is applied across the electrodes, the IPMC material bends. The bending is caused by induced swelling on the cathode side of the material and shrinking on the anode side due to a sudden flux of cations and polar solvent. By applying a voltage with opposite polarity, bending in the opposite direction occurs. In addition, when an IPMC is mechanically deformed, charges develop across the electrodes and thus IPMCs can function as a sensor [20].

The IPMC tube actuator is fabricated from a Nafion polymer tube (Global FIA) with inner diameter of 1.3 mm and outer diameter of 1.6 mm. Figure 2 shows the principle of operation for the tube-shaped IPMC actuator when voltage is applied, specifically for straight and diagonal deformation.

The fabrication process involves five major steps: (1) surface treatment, (2) ion exchange, (3) reduction, (4) surface electroding, and (5) surface machining. Each process is briefly described below, where the Nafion tube is plated with platinum electrode by following the process described in [21].

(1) Surface Treatment First, the outer surface of the Nafion polymer tube is abraded to enhance the electrode plating process. The surface is abraded using fine-grit sandpaper (ISO grit size P1000). Following the abrading process, the tube is chemically cleaned in a solution of 1 M sulfuric acid, then cleaned again in two baths of deionized water at a temperature of 65°C for 45 minutes.

(2) Ion Exchange Next, the prepared and cleaned Nafion tube is submerged in a complex platinum solution (0.2 M [Pt(NH₃)₄]Cl₂) at room temperature for ion exchange. The platinum solution with the tube is stirred for approximately three hours.

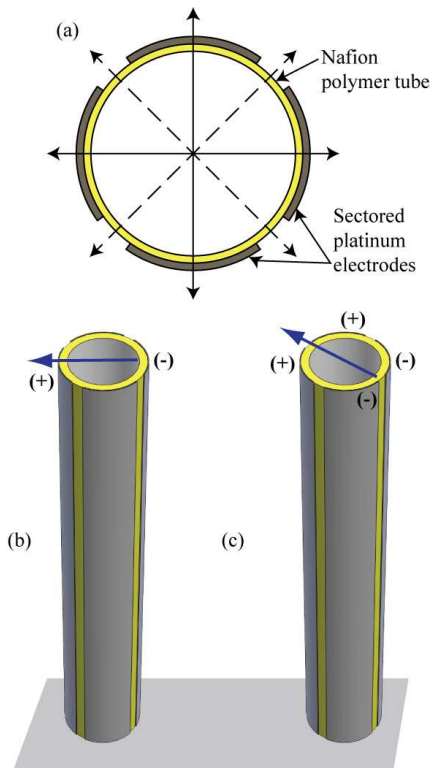


FIGURE 2. The IPMC tube actuator: (a) electrode configuration (top view), (b) electrode charge patterns for straight direction of movement and (c) electrode charge patterns for diagonal direction of moment. Arrows indicate the direction of deformation.

(3) Reduction Then, the primary platinum plating is reduced to its metallic state with a reducing agent. The tube is immersed in deionized water at 65°C and 0.2 g of sodium borohydride is added every half hour for three hours. The surface of the tube turns dark gray in color due to the presence of platinum metal. Chemical cleaning as described in the first step followed this process.

(4) Electrode plating After the primary plating, a secondary plating is added, where platinum is deposited on the surface to decrease surface resistivity. A platinum solution is prepared and heated to 50°C before the tube is submerged in the solution. While stirring, 2 mL of 5% hydroxylamine hydrochloride and 1 mL of 20% hydrazine monohydrate is added every half hour for three hours while gradually elevating the temperature to 65°C . The IPMC is then placed in a solution of 1 M lithium chloride at room temperature for 24 hours for ion exchange.

(5) Electrode machining After the electrode plating process, the electrode on the outer surface of the tube is sectored into four isolated regions using a surface machining process. The machining process is illustrated in Fig. 3, where a computer-controlled milling machine equipped with a small mill tool is used to remove a thin layer (approximately 50 to 80 μm thick) of platinum

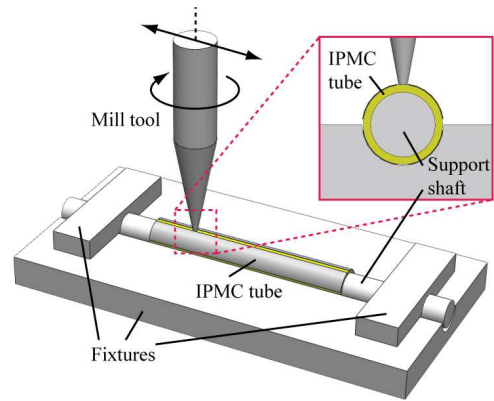


FIGURE 3. Electrode surfacing milling process for tube-shaped IPMC actuator. IPMC tube is held in place using fixtures, and a milling tool removes the electrode material.

from the surface of the polymer. The mill tool rotates at approximately 2000 RPM and the milling process is performed with liquid coolant to prevent heating effects.

3 Integrated Strain Sensor

Displacement sensing for IPMC actuators is critical for active control and validating system models. Popular sensors include lasers [22], CCD cameras [23], or force sensors [24], which may or may not come into physical contact with the actuator, to measure the IPMC's response. The most commonly used are laser displacement sensors which are relatively inexpensive and the light beam can penetrate water as well as many types of transparent layers, such as acrylic plastic. Practically speaking, however, laser systems are bulky and the output can vary with surface reflectivity, thus precluding their use in small and lightweight autonomous systems. More compact sensors include bonding PVDF thin films to the surface of an IPMC actuator [25]. Additionally, the mechano-electrical transduction ability of IPMC materials can be exploited to create IPMC-based sensors [20]. For example, an IPMC actuator with patterned electrodes for self-sensing has been proposed [18, 26]. This method involves creating two isolated regions of the composite material, one for actuation and one for sensing deformation. The self-sensing approach is compact; however, the major challenges are ensuring that the actuating and sensing electrodes are properly isolated to overcome feedthrough or cross-coupling issues [18, 27] and accounting for sensor nonlinearity [20].

Recently, resistive strain sensors were used for sensing IPMC deformation [9]. The main advantages of strain gage sensors are they are compact, flexible, and they can easily be bonded to the surface of an actuator. Resistive strain gages are made of either an insulated small-diameter wire or thin layer of conducting foil encapsulated in an insulating material. When used with an IPMC actuator, the insulated packaging eliminates cross-

coupling effects between the applied voltage to the IPMC electrodes and the attached strain gage.

To sense the deformation of the IPMC tube actuator, a resistive strain sensor is developed using a 50 AWG ni-chrome (20% nickel and 80% chrome) wire. The wire is chosen because of its small size and its desired material properties, namely resistivity ρ , as shown in Table 1. The wire is available with an insulating sheath, and thus when the wire is bonded to the electrode of an IPMC, the insulation eliminates any feedthrough from the IPMC control voltage to the sensor output.

Figure 4 shows the details of the resistive strain sensor, signal condition circuit, and an example of an experimental IPMC tube actuator with the wire strain sensor bonded to its outer surface. As the actuator deforms, the sensor experiences a strain which changes the wire's overall resistance. This change in resistance is detected through an imbalance in the Wheatstone bridge circuit. Under certain conditions, the change in resistance of the strain sensor is linearly related to the bending deformation of the tube actuator. Multiple sensors can be placed on the actuator to detect displacement in multiple directions.

TABLE 1. Electrical and mechanical properties of a 50 AWG ni-chrome wire.

Property	Symbol	Value
Resistivity	ρ	$100 \times 10^{-8} \Omega/\text{m}$
Cross-sectional area	A	0.001963 mm^2
Poisson's ratio	ν	0.38

An approximation of the change in resistance ΔR of the wire strain sensor to the displacement δ of the end of the tube actuator when the tube is fixed at one end is given by

$$\Delta R = \frac{3D\rho L_w \delta}{2A} \left(\frac{1+2\nu}{L_t^2 - 3\delta D\nu} \right), \quad (1)$$

where D and L_t are outer diameter and length of the IPMC tube, respectively; and L_w , ρ , A , and ν are the length, resistivity, cross-sectional area, and Poisson's ratio of the wire sensor, respectively.

The small changes in resistance corresponding to strain is detected by the Wheatstone quarter-bridge circuit shown in Fig. 4. The output voltage of the bridge circuit, V_1 , as a function of the unit change in resistance, $\Delta R/R$, of the strain gage is given by

$$V_1 = \left(\frac{\Delta R/R}{2} \right) \left(\frac{1}{2 + \Delta R/R} \right) V_s, \quad (2)$$

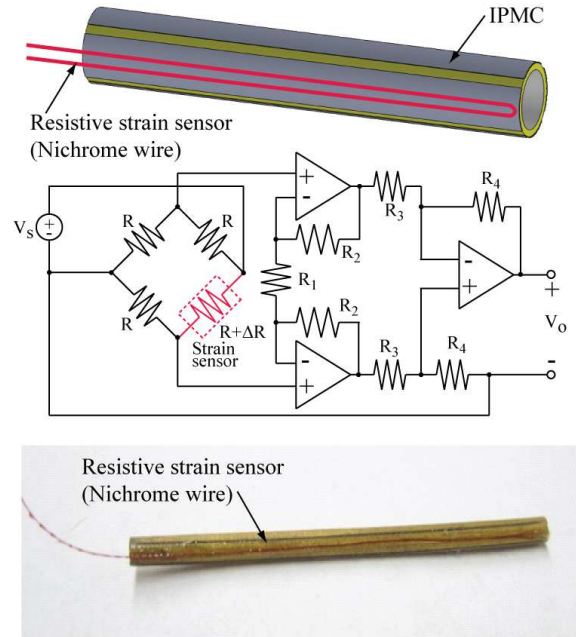


FIGURE 4. Resistive strain sensor attached to outer surface of IPMC tube actuator for sensing deformation. A Wheatstone bridge and amplifier circuit are used for signal conditioning. V_s and V_o are the source and output voltages, respectively.

where V_s is the gage-excitation voltage. The gage-excitation voltage is kept relatively low (≤ 3 V) to avoid self-heating which can degrade the performance of the gage. Neglecting the bridge non-linearity, the change in the output voltage as a function of the unit change in resistance is

$$V_1 = \frac{1}{4} \left(\frac{\Delta R}{R} \right) V_s. \quad (3)$$

As shown in Fig. 4, the bridge voltage is amplified by a differential amplifier, resulting in an output voltage of

$$V_s = \frac{1}{4} \left[\frac{R_4}{R_3} \left(\frac{2R_2}{R_1} + 1 \right) \right] \left(\frac{\Delta R}{2R} \right) V_s. \quad (4)$$

4 Preliminary Results and Discussion

Scanning electron microscope (SEM) images revealing details of the IPMC tube actuator are shown in Fig. 5. In particular, an image of the cross-section of the tube showing the polymer material and platinum electrode is presented in Fig. 5(a). The platinum electrode layer is approximately 15 to 25 μm thick. Figure 5(b) shows the cross section of the milled surface, where the milled feature is approximately 80 μm deep and 170 μm wide. The details of the edge of the feature, viewed perpendicular to the electrode surface, is shown in Fig. 5(c). As can be seen,

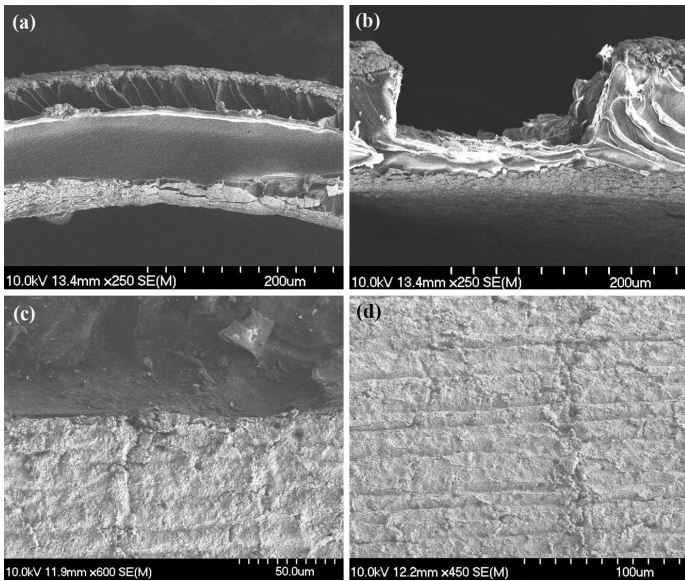


FIGURE 5. SEM images of IPMC tube actuator: (a) cross section of tube, (b) cross section of milled surface, (c) top view of edge of milled surface, and (d) surface of platinum electrode.

the sharp contrast between the light and dark color in the image indicates that the platinum electrode is completely removed by the mill tool. A close-up view of the platinum electrode itself is shown in Fig. 5(d).

Experiments are performed to demonstrate the performance of the IPMC tube-shaped actuator and integrated strain sensor. Figure 6 shows the experimental IPMC tube actuator (length of 40 mm, outer diameter of 1.6 mm and inner diameter of 1.3 mm) submerged in deionized water. The tube is fixed at one end and the free end (points downward) is free to move in water. Electrical power to actuate the IPMC tube is delivered to each set of electrodes via a four-point electrical connector. The experimental system also consists of a custom-designed voltage amplifier [9], computer and data acquisition system, signal conditioning circuitry, and video camera (not shown in Fig.6).

The bending performance of the IPMC tube actuator is qualitatively evaluated by recording the motion using a video camera. The camera is positioned such that it is focused on the free end of the tube, and the camera's lens is perpendicular to the axial direction of the tube actuator. Voltages are applied to opposing pairs of electrodes to actuate the tube in two directions (x and y). From the video results, images showing the maximum displacement of the free end of the tube are shown in Fig. 7, where the maximum displacement along the x and y directions is approximately ± 3 mm. As can be seen, the bending motion of the IPMC tube actuator can be controlled in two directions. Due to the asymmetry of the electrode sectors (caused by manufacturing errors) as well as inhomogeneity of the material characteristics, the bending motion is not orthogonal and noticeable cross-coupling effects can be observed. For example, the IPMC tube is driven

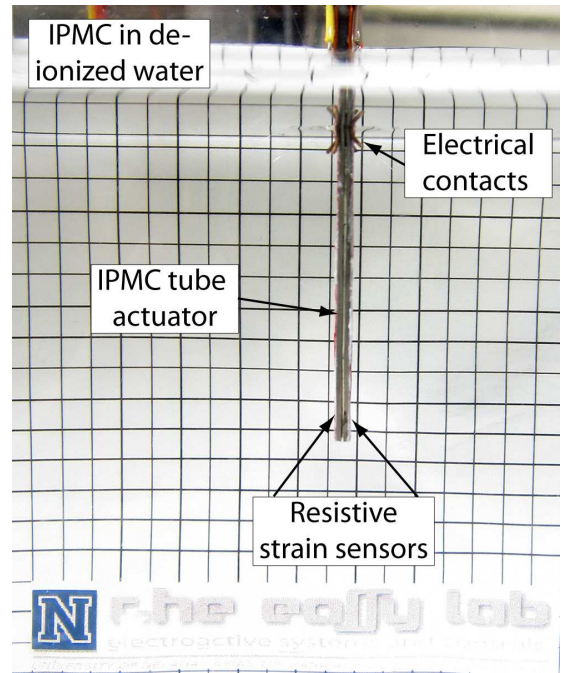


FIGURE 6. The experimental IPMC tube actuator submerged in deionized water. Electrical power to actuate the IPMC tube is delivered to each set of electrodes via a four-point electrical connector.

in the $+x$ direction by driving two opposing electrodes; however, the resulting motion shows components in the $+x$ and $-y$ directions as illustrated in Fig. 7.

The response of a resistive strain sensor attached to one electrode where the tip of the tube experiences a displacement of ± 2 mm is shown in Fig. 8. Two input signals were applied to deflect the tube: a sinusoidal and a triangular input signal, both signals applied at a frequency of 0.1 Hz and 1 Hz. As shown in Fig. 8, the strain sensor's output response (measured in volts) corresponds to the input signal that deflects the tube actuator. Thus, the strain sensor is able to sense the bending motion of the tube actuator, and the sensor signal can be used for feedback control purposes.

5 Conclusions and Future Work

This paper described the development of a tube-shaped ionic polymer-metal composite (IPMC) actuator with sectored electrodes. The tube-shaped actuator is manufactured from a Nafion polymer tube, and the plated platinum electrodes were sectored into four isolated electrodes using a simple surface milling process. A custom-designed strain sensor comprised of 50 AWG ni-chrome wire is developed and attached to the tube's surface to sense the bending motion of the tube actuator. Experimental results were presented to demonstrate the performance of the IPMC tube actuator and integrated displacement sensor.

Future work includes (1) improving the manufacturing pro-

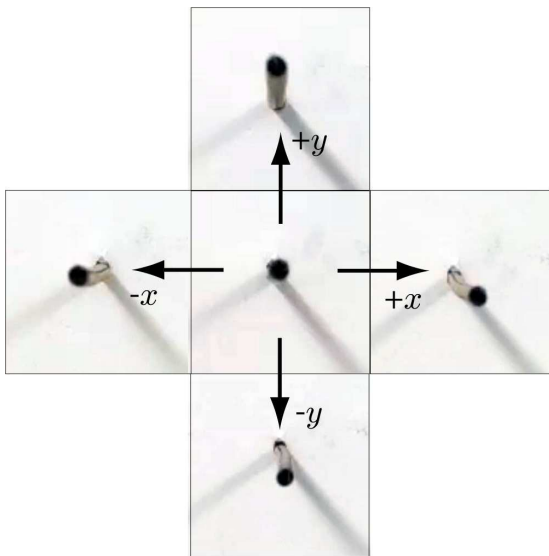


FIGURE 7. IPMC tube actuator bending motion. Actuator is oriented such that it points out of the plane of the paper.

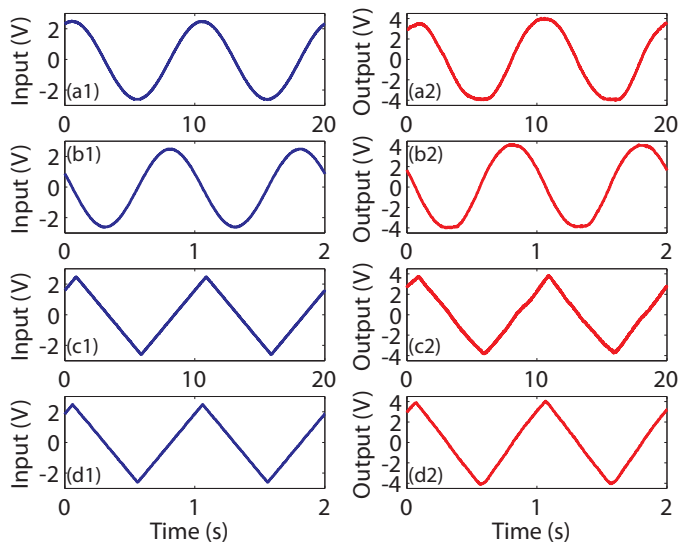


FIGURE 8. Measured resistive strain sensor time responses where the IPMC tube's tip displacement is ± 2 mm: (a1) input and (a2) output for 0.1 Hz sinusoidal signal; (b1) input and (b2) output for 1 Hz sinusoidal signal; (c1) input and (c2) output for 0.1 Hz triangle signal; and (d1) input and (d2) output for 1 Hz triangle signal. Results were measured with IPMC in deionized water.

cess to produce more symmetric electrode patterns to minimize cross-coupling effects during actuation; (2) integrating multiple strain sensors for sensing the displacement of the tube actuator along multiple directions; and (3) exploiting the strain sensor signal for feedback control to compensate for disturbances and nonlinearities.

6 Acknowledgements

Authors acknowledge financial support from the Office of Naval Research, grant number N00014-13-1-0274.

REFERENCES

- [1] Shahinpoor, M., and Kim, K., 2004. "Ionic polymer-metal composites: IV. Industrial and medical applications". *Smart Materials and Structures*, **14**, August, pp. 197–214.
- [2] Feng, G., and Tsai, J., 2011. "3D omnidirectional controllable elastic IPMC tweezer with self-sensing and adjustable clamping force abilities for biomedical applications". *Proc. Transducers '11*, **18**, pp. 1725–1728.
- [3] Kamamichi, N., Yamakita, M., Asaka, K., and Luo, Z.-W., 2006. "A snake-like swimming robot using IPMC actuator/sensor". *Proc. Conf. on Rob. and Auto.*(Orlando, Florida), pp. 1812–1817.
- [4] Arena, P., Bonomo, C., Fortuna, L., Frasca, M., and Graziani, S., 2007. "Design and control of an IPMC worm-like robot". *Cybernetics*, **36**, pp. 1044–1052.
- [5] Nguyen, T., Goo, N., Nguyen, V., Yoo, Y., and Park, S., 2008. "Design, fabrication, and experimental characterization of a flap valve IPMC micropump with a flexibly supported diaphragm". *Sensors and Actuators: A. Physical*, **141**, pp. 640–648.
- [6] Chen, Z., Shatarra, S., and Tan, X., 2010. "Modeling of biomimetic robotic fish propelled by an ionic polymer-metal composite caudal fin". *IEEE/ASME Transactions on Mechatronics*, **35**, pp. 448–459.
- [7] Palmre, V., Fleming, M., Hubbard, J. J., Pugal, D., Kim, S., Kim, K. J., and Leang, K. K., 2013. "An IPMC-enabled bio-inspired bending/twisting fin for underwater applications". *Smart Materials and Structures*, **22**, p. 014003.
- [8] Yong, Y. K., Arain, B., and Moheimani, S. O. R., 2010. "Atomic force microscopy with a 12-electrode piezoelectric tube scanner". *Review of Scientific Instruments*, **81**(3), p. 033701.
- [9] Leang, K., Shan, Y., Song, S., and Kim, K., 2012. "Integrated sensing for IPMC actuators using strain gages for underwater applications". *IEEE/ASME Transactions on Mechatronics*, **17**(2), pp. 345–355.
- [10] Aureli, M., Kopman, V., and Porfiri, M., 2010. "Free-locomotion of underwater vehicles actuated by ionic polymer metal composites". *IEEE/ASME Trans. Mechatronics*, **15**(4), pp. 603 – 614.
- [11] Yim, W., Lee, J., and Kim, K. J., 2007. "An artificial muscle actuator for biomimetic underwater propulsors". *Bioinsp. Biomim.*, **2**, pp. S31 – S41.
- [12] Lee, S., Han, M., Kim, S., Jho, J., Lee, H., and Kim, Y., 2006. "A new fabrication method for IPMC actuators and application to artificial fingers". *Smart Materials and Structures*, **15**, pp. 1217–1224.

- [13] Bonomo, C., Bottino, M., Brunetto, P., Pasquale, G. D., Fortuna, L., Graziani, S., and Pollicino, A., 2010. "Tridimensional ionic polymer metal composites: optimization of the manufacturing techniques". *Smart Materials and Structures*, **19**(055002).
- [14] Shan, Y., and Leang, K. K., 2009. "Frequency-weighted feedforward control for dynamic compensation in ionic polymer-metal composite actuators". *Smart Materials and Structures*, **18**(12), p. 125016 (11 pages).
- [15] Kim, K. J., Pugal, D., and Leang, K. K., 2011. "A twistable ionic polymer-metal composite artificial muscle for marine applications". *Marine Technology Society Journal*, **45**(4), pp. 83 – 98.
- [16] Tiwari, R., and Kim, K. J., 2010. "Disc-shaped ionic polymer metal composites for use in mechano-electrical applications". *Smart Materials and Structures*, **19**, p. 065016.
- [17] Kim, S. J., Pugal, D., Wong, J., Kim, K. J., and Yim, W., 2013. "A bio-inspired multi degree of freedom actuator based on a novel cylindrical ionic polymer-metal composite material". *Robotics and Autonomous Systems (In press)*.
- [18] Kruusamae, K., Brunetto, P., Graziani, S., Punning, A., Di Pasquale, G., and Aabloo, A., 2009. "Self-sensing ionic polymer-metal composite actuating device with patterned surface electrodes". *Polymer International*, **59**(3), pp. 300 – 304.
- [19] Shahinpoor, M., and Kim, K., 2001. "Ionic polymer-metal composites: I. Fundamentals". *Smart Materials and Structures*, **10**, March, pp. 819–833.
- [20] Pugal, D., Jung, K., Aabloo, A., and Kim, K. J., 2010. "Ionic polymermetal composite mechano-electrical transduction: review and perspectives". *Polymer International*, **59**(3), pp. 279 – 289.
- [21] Shahinpoor, M., and Kim, K., 2003. "Ionic polymer-metal composites: II. Manufacturing techniques". *Smart Materials and Structures*, **12**, August, pp. 65–79.
- [22] Lin, H.-H., Fang, B.-K., Ju, M.-S., and Lin, C.-C. K., 2009. "Control of ionic polymer-metal composites for active catheter systems via linear parameter-varying approach". *Journal of Intelligent Material Systems and Structures*, **20**(3), pp. 273 – 282.
- [23] Lavu, B. C., Schoen, M. P., and Mahajan, A., 2005. "Adaptive intelligent control of ionic polymermetal composites". *Smart Materials and Structures*, **14**(4), pp. 466 – 474.
- [24] Bhat, N. D., and Kim, W.-J., 2004. "Precision force and position control of ionic polymer-metal composite". *Journal of Systems and Control Engineering*, **218**(6), pp. 421 – 432.
- [25] Chen, Z., Ki-Yong, K., and Tan, X., 2008. "Integrated IPMC/PVDF sensory actuator and its validation in feedback control". *Sensors and Actuators: A. Physical*, **144**(2), pp. 231 – 241.
- [26] Alici, G., Spinks, G. M., Madden, J. D., Wu, Y., and Wallace, G. G., 2008. "Response characterization of electroactive polymers as mechanical sensors". *IEEE/ASME Trans. Mechatronics*, **13**(2), pp. 187 – 196.
- [27] Punning, A., Kruusmaa, M., and Aabloo, A., 2007. "A self-sensing ion conducting polymer metal composite (IPMC) actuator". *Sensors and Actuators: A. Physical*, **136**, pp. 656 – 664.